The original publication is available at www.springerlink.com
DOI: 10.1023/A:1014943312031

Regular paper

Excitation energy transfer in chlorosomes of *Chlorobium phaeobacteroides* strain CL1401: The role of carotenoids

Jakub Pšenčík[1#], Ying-Zhong Ma[2†], Juan B. Arellano[1,3‡], Jesús Garcia-Gil[3], Alfred R. Holzwarth[2] and Tomas Gillbro[1]

[1]Department of Chemistry, Biophysical Chemistry, Umeå University, S-901 87 Umeå, Sweden; [2]Max-Planck-Institut für Strahlenchemie, Stiftstr. 34-36, D-45470 Mülheim a.d. Ruhr, Germany; [3]Laboratory of Microbiology, Institute of Aquatic Ecology, University of Girona, Campus de Montilivi, Girona, Spain; [#]On leave from Department of Chemical Physics and Optics, Faculty of Mathematics and Physics, Charles University, Ke Karlovu 3, 121 16 Prague 2, Czech Republic; [†]Present address: Department of Chemistry, University of California, Berkeley, California 94720-1460. [‡]Present address: Instituto de Recursos Naturales y Agrobiologia (CSIC), Cordel de Merinas 52, 37008 Salamanca, Spain

Address for correspondence:
Jakub Pšenčík
Department of Chemical Physics and Optics
Faculty of Mathematics and Physics
Charles University
Ke Karlovu 3
CZ-121 16 Praha 2
Czech Republic

tel. +420 2 2191 1307
fax +420 2 2191 1249
e-mail: jakub.psencik@mff.cuni.cz

Key words: carotenoid, bacteriochlorophyll, chlorosome, *Chlorobiaceae*, energy transfer, femtosecond spectroscopy, fluorescence excitation, green sulfur bacteria, single-photon timing

Abstract

The role of carotenoids in chlorosomes of the green sulfur bacterium *Chlorobium phaeobacteroides*, containing bacteriochlorophyll (BChl) *e* and the carotenoid (Car) isorenieratene as main pigments, was studied by steady-state fluorescence excitation, picosecond single-photon timing and femtosecond transient absorption (TA) spectroscopy. In order to obtain information about energy transfer from Cars in this photosynthetic light-harvesting antenna with high spectral overlap between Cars and BChls, Car-depleted chlorosomes, obtained by inhibition of Car biosynthesis by 2-hydroxybiphenyl, were employed in a comparative study with control chlorosomes. Excitation spectra measured at room temperature give an efficiency of 60-70% for the excitation energy transfer from Cars to BChls in control chlorosomes. Femtosecond TA measurements enabled an identification of the excited state absorption band of Cars and the lifetime of their S_1 state was determined to be ~10 ps. Based on this lifetime, we concluded that the involvement of this state in energy transfer is unlikely. Furthermore, evidence was attained for the presence of an ultrafast (<100 fs) energy transfer process from the S_2 state of Cars to BChls in control chlorosomes. Using two time-resolved techniques, we further found that the absence of Cars leads to overall slower decay kinetics probed within the Qy band of BChl *e* aggregates, and that two time constants are generally required to describe energy transfer from aggregated BChl *e* to baseplate BChl *a*.

Abbreviations: BChl - bacteriochlorophyll, Car - Carotenoid, *Cfl.* - *Chloroflexus*, *Chl.* - *Chlorobium*, DAS - decay associated spectrum, ESA -excited state absorption, FWHM - full-width at half maximum, PB/SE - photobleaching/stimulated emission, SPT - single-photon timing, TA - transient absorption

Introduction

Chlorosomes are the major light-harvesting antennae of green filamentous and green sulfur bacteria, consisting of several thousand bacteriochlorophyll (BChl) *c*, *d* or *e* molecules in the

form of self-aggregates (Blankenship et al. 1995). Minor amounts of BChl *a* are also present in chlorosomes, amounting to a few percent of the aggregated BChls, to form the baseplate which interfaces the chlorosomes to the membrane (Blankenship et al. 1995). In addition, chlorosomes also contain a variable amount of carotenoids (Cars), depending on the species (Liaaen-Jensen 1965; Schmidt 1980; Oelze and Golecki 1995). *Chlorobium (Chl.) phaeobacteroides* contain mainly the carotenoids isorenieratene and β-isorenieratene. The stoichiometric ratio between BChls and Cars vary from 20:1 to 2:1 for the genus *Chlorobium* (Borrego and Garcia-Gil 1995) and, for green bacteria in general, is influenced considerably by the growth conditions. It was observed for *Chloroflexus* (*Cfl.*) *aurantiacus* that an increased light intensity leads to an increasing content of Cars in the chlorosomes (Ma et al. 1996), while for the genus *Chlorobium* the effect is much less pronounced and appears instead as a decrease of ~10% (Borrego and Garcia-Gil 1995). This was accompanied by a blue shift of the main BChl Q_y band, due to changes in the main homologues (Borrego and Garcia-Gil 1995). The location and function of Cars in green bacteria have not been well defined yet and is a subject of intensive study. Recently, Car-deficient chlorosomes were prepared and characterized for both green filamentous (Foidl et al. 1997; Frese et al. 1997) and green sulfur bacteria (Arellano et al. 2000). Based on these results, it has been suggested that Cars are located in the vicinity of BChls and probably play a role in protection against photo-oxidation and structural stabilization of baseplate BChl *a*. The close interaction between Cars and BChls has been also proposed previously, as a requirement for BChl→ Car triplet-triplet energy transfer (Psencik et al. 1994a). For *Cfl. aurantiacus* it was deduced that organization of BChl *c* aggregates is largely independent of Cars (Freese et al. 1997). However, in the case of *Chl phaeobacteroides*, Car-inhibition was found to affect presumably the organization of BChl *e*, while the arrangement of BChl *a* seems not be affected (Arellano et al 2000).

The light harvesting function of Cars has been studied so far mainly on the basis of steady-state fluorescence excitation spectra. An efficiency of Car→BChl energy transfer was

estimated to be 65% for *Cfl. aurantiacus* at 4 K (van Dorssen et al. 1986), 90-100% for isorenieratene-containing *Chl phaeovibrioides* at 6 K (Otte et al. 1991) and 50-80% for *Cfl. aurantiacus and Chl. tepidum* at 300 K (Melø et al. 2000). In contrast, only 15% efficiency of Car→BChl energy transfer in chlorosomes of *Chl phaeobacteroides* has been found by Aschenbrücker et al. (unpublished data) who argued that the bacteria have access to light in the region around 500 nm via the unusually structured Soret band of aggregated BChl *e*. It is unclear whether the differences in energy transfer efficiencies of Cars are due to intrinsic properties of chlorosomes, growth conditions or isolation artifacts. In contrast to e.g. purple bacteria (e.g. Macpherson et al. 2001), a direct study of Car→BChl energy transfer by time-resolved techniques is complicated by the large spectral overlap between the BChl Soret band and Car absorption. The main absorbing state of Cars is the S_2 state with a lifetime of 120-177 fs for β-carotene (having the same length of the polyene chain as isorenieratene) in solution (Macpherson and Gillbro 1998). The optically forbidden S_1 state with a lifetime of ~10 ps for β-carotene (Andersson et al. 1995) can be populated via internal relaxation from the S_2 state. An involvement of S_1 and S_2 states in energy transfer for various photosynthetic complexes is a matter of debate. If either S_1 or S_2 state is involved in the excitation energy transfer to BChls a significant shortening of the respective lifetime is expected.

Excitation energy transfer in chlorosomes has been extensively studied using various spectroscopic techniques in the last decade (see review by Blankenship et al. 1995 and related references therein; Psencik et al. 1994b; Savikhin et al. 1995; Mimuro et al. 1996; Ma et al. 1996; Savikhin et al. 1996a; Savikhin et al. 1996b; Psencik et al. 1998; van Walree et al. 1999; Steensgaard et al. 2000; Prokhorenko et al. 2000). The transfer step from aggregated BChls to the baseplate is probably the best characterized process. In earlier studies it has been found that this transfer can be described by a single time constant as revealed by picosecond time-resolved fluorescence and transient absorption (TA) experiments, with a value depending on the species (Holzwarth et al. 1990; Miller et al. 1991; Causgrove et al. 1992), growth conditions of the bacteria (Ma et al. 1996; Fetisova et al.

1996) and redox states (Causgrove et al. 1990; Wang et al 1990; van Noort et al. 1997). However, a more recent study on the isolated chlorosomes from *Chl. phaeobacteroides* and *Chl. tepidum* showed that two time constants are required to describe this transfer process (van Walree et al. 1999). This result was obtained by a global lifetime analysis of the kinetics detected using picosecond single-photon timing (SPT). Two of the resulting decay-associated-spectra (DAS) are characterized by amplitudes with opposite signs in the BChl *c*/*e* and BChl *a* emission regions. However, due to the low spectral resolution of the DAS, in particular for the measurements done on the chlorosomes from *Chl. phaeobacteroides*, it is hard to distinguish any difference in the corresponding DAS. A better resolved DAS, however, would be useful to understand the details of these transfer processes.

In this study, we applied femtosecond TA and picosecond SPT techniques in a systemic investigation of control and Car-depleted chlorosomes from *Chl. phaeobacteroides*. This enabled a separation and characterization of the contribution of Cars to the measured kinetics. The analyses of the kinetics also confirmed that two time constants are required to describe the excitation energy transfer process from the aggregated BChl *e* to the baseplate.

Materials and Methods

Sample Preparation: Growth of cells and isolation of chlorosomes were carried out as described previously (Arellano et al. 2000), and samples were kept at –20°C until use. In Car-inhibited chlorosomes Car biosynthesis were inhibited by more than 95% by 2-hydroxybiphenyl, leading to an accumulation of the colorless precursor phytoene inside the chlorosomes (Arellano et al. 2000). All TA experiments were performed on isolated chlorosomes diluted with 50 mM Tris-HCl buffer (pH 8.0) containing 2 M NaSCN to an absorbance from 0.5 to more than 3.0 per mm at the respective BChl *e* Q_y maxima, depending on the pump/probe wavelengths. 1 mm glass cuvettes were used and the chlorosomes were incubated with 20 mM sodium dithionite for 2 h before the measurement to achieve anaerobic conditions. The same procedure, except for an absorbance of 0.1-0.2

per 1 cm and use of a 1 cm glass cuvette, was employed for the measurement of fluorescence excitation spectra. For the SPT experiment, the samples were diluted to an absorbance of ~0.2-0.3 per cm at each excitation wavelength using a 20 mM potassium phosphate buffer (pH 7.4) containing 2 M NaSCN. A total volume of 25-40 ml sample was prepared and pumped through a fluorescence cuvette with a 1.5×1.5 mm^2 optical cross section at a speed of 10 ml/min. To ensure anaerobic conditions, we used the procedure described previously (van Walree et al. 1999), except the concentration of sodium dithionite was 20 mM. The integrity of the samples was controlled by measurements of absorption spectra before and after both TA and SPT experiments. Additionally, steady-state fluorescence emission spectra were recorded before and after the SPT measurements and the largest change of the emission intensity was found to be less than 15%.

Fluorescence excitation spectra: Steady-state fluorescence excitation spectra were recorded using a SPEX Fluorolog 112 fluorometer equipped with Glan-Thompson polarizers and a Hamamatsu R928 red-sensitive multialkali photomultiplier. The bandwidths for the excitation and emission monochromators were 5.5 and 2.7 nm, respectively. A correction file generated from excitation spectra of selected laser dyes was used to correct the excitation spectra (Macpherson et al. 2001).

Femtosecond TA: Two-color femtosecond TA kinetics were measured using a set-up based on a mode-locked Ti:sapphire femtosecond oscillator (Tsunami, Spectra Physics) together with a Ti:sapphire regenerative amplifier (Spitfire, Positive Light) producing ~100 fs pulses centered around 800 nm at a repetition rate of 5 kHz. The output of the amplifier was split and the major part was used for pump pulse generation by frequency conversion in an optical parametric amplifier (OPA 800, Spectra Physics) to desired excitation wavelengths (505, 675 or 685 nm). 505 nm pulses were further compressed by two SF14 prisms. Pulses of $\lambda \geq 675$ nm were used without any further compression. A white-light continuum generated in a sapphire plate by the minor part of the amplifier output was used as a probe pulse. The relative polarization of the pump beam with respect to the probe beam was set to the magic

angle, 54.7°, by a Berek compensator (New Focus, Model 5540). The desired probe wavelength was selected after passing a monochromator with a bandwidth of 5 nm. Absorption changes were detected by silicon photodiodes. Excitation intensity was between $5 \cdot 10^{11}$-$5 \cdot 10^{13}$ photons·cm^{-2}·pulse^{-1} and the spot size of the pump beam at the sample place was 0.5-0.7 mm. The cross correlation between the pump and probe pulses was ~150 fs and ~200 fs (full-width at half maximum, FWHM) for the pump wavelengths at 505 and ≥ 675 nm, respectively. TA spectra were measured by scanning the monochromator while simultaneously adjusting the time delay to compensate for the white-light dispersion, the so-called chirp correction. The kinetics were analyzed by the Spectra program using a model function consisting of a Gaussian response convoluted with multiple exponentials.

Picosecond SPT: Time-resolved fluorescence measurements were performed using a picosecond SPT apparatus set at the magic angle polarization. A cavity-dumped dye laser system synchronously pumped by a mode-locked Ar^+ laser was used as an excitation source. Pyridine-1 was used as the laser dye to generate pulses between 670-740 nm with a typical duration of 10 ps at a repetition rate of 4 MHz. Excitation was at 710 and 730 nm with a pulse energy of ~1 nJ. Fluorescence emission was selected by using a near-infrared double grating monochromator (DH10 VIR, Jobin Yvon) with a bandwidth of 4 nm and detected with a cooled infrared sensitive microchannel plate photomultiplier (Hamamatsu R3809U-51). The instrumental response function had a FWHM of ~35 ps. A channel resolution of 2.78 ps was chosen and typically more than 10 000 counts were collected in the peak channel in order to obtain a good signal-to-noise ratio.

Results

Excitation and 1-T spectra: **Figure 1** shows absorption (1-T) spectra of control and Car-inhibited chlorosomes of *Chl. phaeobacteroides*, together with the corresponding fluorescence excitation spectra detected at 810 nm (emission of BChl *a*). The excitation spectra were scaled according to the Q_y absorption maxima of BChl *e*. Almost identical

results (not shown) were obtained at the detection wavelength 745 nm, where the emission of BChl *e* is monitored. Absorption maxima of the BChl *e* Q_y band are at 704 and 714 nm for Car-depleted and control chlorosomes, respectively. Absorption maxima in the blue-green part of spectra (~460 and ~520 nm) do not differ significantly for the two types of chlorosomes. There is excellent agreement between absorption and excitation spectra for Car-deficient chlorosomes. For control chlorosomes a clear difference between the excitation and absorption spectra can be observed in the spectral region 425-525 nm, indicating a less than 100% efficiency of energy transfer from Cars to BChls.

TA spectra: **Figure 2** shows TA spectra in the spectral region 510-700 nm upon excitation at 505 nm. This wavelength is close to the maximum of the lowest vibrational level of the Car $S_0 \rightarrow S_2$ transition, as judged from the difference between absorption spectra of control and Car-depleted chlorosomes (Arellano et al. 2000) and also from the difference spectrum in Figure 1. Both the TA spectra exhibit a negative band due to photobleaching and/or stimulated emission (PB/SE), peaking at ~540 nm. At longer probe wavelengths, both TA spectra show a broad region of positive signal due to excited state absorption (ESA). For Car-inhibited chlorosomes, the ESA is characterized by two maxima at 610 and 670 nm, which are essentially unchanged for the TA spectra detected at different delay times. In the case of control chlorosomes, the feature of the ESA clearly changes with delay time, accompanied by an obvious blue-shifted isosbestic point. The TA spectrum measured at 100 fs shows two maxima peaking at 610 and 680 nm, respectively. The former is replaced by a maximum at 590 nm in the TA spectrum detected at 500 fs. We attribute the 590 nm band to the ESA from the S_1 state of Cars, and the band at 680 and 670 nm observed in the control and Car-inhibited chlorosomes, respectively, to the ESA of BChl *e* aggregates (see Discussion).

The time evolution of the TA spectrum is very fast. Between 510 and 570 nm it basically follows the pump pulse, reaching its maximal amplitude at around 100 fs, which then decays very rapidly. This decay is observable by comparing the TA spectra detected at 100 and 500 fs and is more pronounced for control chlorosomes. Between 570 and 700 nm

the maximal amplitudes are reached within the first 1 ps. As can be seen in detail from the kinetics measured at the corresponding probe wavelengths (Figure 3, bottom panel), the ESA maximum at 590 nm is reached at ~300 fs (with a progressive blue shift) and the maximum around 670-680 nm at ~700 fs (with a progressive red shift). The TA spectra detected at later times (≥1 ps) show a relatively slow decay at all wavelengths (not shown).

TA kinetics between 500 and 700 nm: To get more detailed information about the time evolution observed in the TA spectra, we measured kinetics upon excitation at 505 nm. The results obtained at the most relevant wavelengths are summarized in **Table 1**. At certain wavelengths, the analysis of the kinetics was complicated by a two-photon absorption-like signal and/or coherent oscillations which often influenced the kinetics at the early times, especially where the TA signal was weak. The top panel of **Figure 3** shows the first 5 ps of the kinetics probed at 540 nm, the maximum of the PB/SE band observed in the TA spectra (see Figure 2). At this wavelength a contribution is expected due to relaxation from the BChl Soret band, which is mixed with Car S_2 relaxation in the case of control chlorosomes. Amplitudes of the TA signal at this wavelength, after normalizing for the same number of absorbed photons, were the same (± 5%) for both chlorosome preparations. However, a striking difference between the kinetics was found in the first few hundred femtoseconds. Both kinetics begin with an ultrafast decay which could be best fitted with a ~50 fs lifetime. Given that the response function of the setup was about 150 fs, the uncertainty in the determined lifetime can be rather large, exceeding the ≤10% error estimated for other determined parameters. Reasonable fits to the data could also be obtained with shorter lifetimes. The amplitude of this fast component is more than 30% smaller for the Car-inhibited chlorosomes (Table 1) and, as with the lifetime, it does not vary with pump intensity within the range ($5\cdot10^{12}$-$5\cdot10^{13}$ photons·cm^{-2}·pulse^{-1}). We further found that it is more complicated to analyze the initial decay of the kinetics probed at other wavelengths within the PB/SE band wherever the TA signal is weak. For instance, at 510-515 nm an additional subpicosecond component with a minor amplitude (~10%) was necessary to fit the data

(Table 1). Nevertheless, the ~50 fs component is always the dominating one and it always has a larger amplitude for the control chlorosomes. For both types of chlorosomes, this amplitude is maximal at the blue edge of the PB/SE band and decreases as the probe wavelength shifts to the red. The subsequent slower decay was found to be clearly dependent on the pump intensity within the whole PB/SE band, and the time constant resolved for the Car-depleted chlorosomes is apparently longer than the corresponding time obtained using the control chlorosomes (Table 1). In addition, the overall decay appears slower with increasing wavelength from 510 to 560 nm. It is interesting to note that if four exponential components were used to fit the data, the two slowest lifetimes are similar to those resolved from the decay kinetics probed within the BChl *e* Q_y band.

The contribution from the Car S_1 state to the ESA signal from control chlorosomes is maximal at around 580 nm. Kinetics probed at this wavelength were only weakly dependent on pump-intensity, in contrast to those measured at the other ESA spectral region where BChl *e* changes are dominant (~680 nm). The time evolution of the S_1 state population begins with a fast ~60 fs rise (Figure 3) and the value of this lifetime is again relatively uncertain. This initial rise is followed by a relatively slow decay, which is dominated by a ~10 ps component. The contribution of this component to the overall decay is maximal at 577 nm, where it has a lifetime of 10.6 ps and contributes 93% of the total amplitude. The kinetics measured for the Car-inhibited chlorosomes differ mainly in the amplitude of the TA signal, which was less 1/3 that of the control chlorosomes (Figure 3) and the decay is slightly slower (Table 1). This smaller amplitude of the TA signal leads to a lower signal to noise ratio and therefore other characteristics of the kinetics, such as a smaller amplitude of the rise, could not be determined with sufficient accuracy. The lifetimes of all decay components become faster and the amplitude A_2 (Table 1) decreases with increasing probe wavelength within this ESA region for both types of chlorosomes. The pump-intensity dependence of the kinetics becomes much stronger at longer wavelengths, indicating a pronounced effect of excitation annihilation. For instance, kinetics at 690 nm were measured for control chlorosomes, and a strong pump-intensity dependence typical for aggregated BChl was

observed. At pump intensities about $1*10^{13}$ photons·cm^{-2}·pulse^{-1} the rise can be observed again, but with a considerably longer time constant (~0.5 ps) than that resolved at 580 nm (Figure 3, bottom panel; Table 1). The subsequent decay can be fitted by two decay components. If instead three components are used, lifetimes similar to those determined in the Q_y band are found, as is also observed at 540 nm (Table 1).

TA kinetics between 700 and 810 nm: Effect of the Car inhibition on the excited state relaxation within BChl Q_y bands was studied both by TA and SPT techniques. In SPT experiments the BChl *e* Q_y band was excited, whereas the TA kinetics for this spectral region were measured upon excitation at both 505 nm and in the BChl *e* Q_y band, and the kinetics measured at a given probe wavelength are similar. TA spectra of control and Car-inhibited chlorosomes measured in this spectral region (not shown) were dominated by a PB/SE band of BChl *e,* peaking at 728 nm and 718 nm, respectively, at delay times ≥1 ps. This 10 nm difference in the TA peak positions, as well as for the corresponding isosbestic points, is similar to the difference seen in the steady state absorption of these two types of chlorosomes. In addition, no peak shift could be resolved in the TA spectra recorded in the BChl *a* region, again in an agreement with the steady-state absorption data. Therefore here we will selectively compare the TA kinetics measured by pumping at the blue edge of BChl *e* Q_y band and probing at the red edge of the BChl *e* and *a* band. The pump wavelength was at 685 and 675 nm for the control and Car-inhibited chlorosomes, respectively, and the corresponding probe wavelength was chosen at 745 and 735 nm in the BChl *e* band and at 810 nm in the BChl *a* band. In contrast to the results obtained in the blue-green spectral region, very strong pump-intensity dependence was found for the kinetics measured in the Q_y spectral region. We further found that pump intensities in the order of 10^{11} photons·cm^{-2}·pulse^{-1} were necessary to reach the condition when this dependence was negligible. A detailed description of the relaxation within BChl *e* and *a* and the annihilation effect will be given in a separate paper. Here we are concerned mainly with the differences between the kinetics measured for control and Car-inhibited chlorosomes at selected wavelengths within

BChl *e* and BChl *a* absorption bands.

Figure 4 and Table 1 summarize the TA results obtained in the Q_y region. The ratio between amplitudes of the TA signal measured in the BChl *e* Q_y band of control and Car-inhibited chlorosomes was close to 1 after normalization for the same number of absorbed photons, (~1.1 for excitation at 505 nm and ~0.85 for excitation in the Q_y band). At low excitation intensities (< $1 \cdot 10^{13}$ photons·cm^{-2}·pulse^{-1}) a subpicosecond intra-chlorosomal process was commonly resolved for the control and Car-inhibited chlorosomes at 745 nm and 735 nm, respectively, manifesting itself as a rise (Figure 4, upper panel). The time constants of this initial rise and the subsequent decay were found to be apparently longer for the Car-inhibited chlorosomes than the control ones (0.42 and 0.51 ps, respectively, for pump intensity $7 \cdot 10^{11}$ photons·cm^{-2}·pulse^{-1}). Although the decay could be fitted by two components with similar lifetimes for both chlorosomes (18.5-20.2 ps, 82-101 ps), in the control chlorosomes the amplitude associated with the faster component is more than twice as large as in the Car-inhibited chlorosomes. In comparison to the data measured in the BChl *e* band, the TA signal within the BChl *a* band was generally smaller, and for control chlorosomes the total amplitude at 810 nm was about 20% of that in the BChl *e* band after excitation at 685 nm. The kinetics measured in the BChl *a* band are very similar for both chlorosomes, except for the difference in their total amplitude. For the Car-depleted chlorosomes, the overall amplitude is only ~40% of the amplitude observed for control chlorosomes (for excitation in the Q_y band). This again led to a low signal/noise ratio and the fitting parameters obtained for the Car-inhibited chlorosomes at 810 nm and under low pump intensities are not very accurate. During the initial ~100 ps, the kinetics for both chlorosomes are dominated by a slow rise, which clearly required two rise components to get a good fit. The lifetime of the faster one agrees well with the faster decay component observed in the BChl *e* band, whereas the second rise component is remarkable slower than the slower decay component of BChl *e* (125-142 ps). Furthermore, this slow rise is followed by a decay, which could be fitted by a single exponential component of 207-221 ps for the limited scan range (600 ps) used in these experiments.

SPT measurement: With respect to the relatively long lifetimes observed in the decay of BChl *e* and BChl *a*, a more detailed comparison between both chlorosome preparations was made with the use of the SPT method. Fluorescence kinetics for both chlorosome preparations were measured at different wavelengths upon excitation at 710 and 730 nm for each preparation, respectively. Global lifetime analyses of all the kinetics detected for each preparation and at each excitation wavelength were performed using a model function consisting of four exponential components, and the corrected wavelength dependence of the resulting amplitudes was plotted as DAS. Data analysis with only three exponential components generally leads to systematic deviations in the weighted residuals, which were also reflected in the global and local chi-square (χ^2) values. The top panel of **Figure 5** shows the DAS obtained using the control chlorosomes upon excitation at 710 nm in a fitting window of 2 ns. Among the four components, those with lifetimes of 33 and 93 ps can be attributed to energy transfer from aggregated BChl *e* to the baseplate BChl *a*, as manifested by a positive amplitude in the BChl *e* emission region as a result of decay and a negative amplitude in the BChl *a* emission band because of a rise term. The DAS associated with these two transfer processes in the BChl *a* emission region are clearly different from one another in their peak positions, and the one with longer transfer time appears to be red-shifted with respect to the one with the shorter lifetime. Upon arriving at the baseplate, the relaxation of equilibrated excitations occurs on two time scales, 310 and 930 ps, respectively, the process with the longer lifetime being dominant.

Kinetics were also measured excitating at 730 nm, where the red-side of the BChl *e* Q_y absorption band is selectively excited. The lifetimes resolved by global analysis are, within the experimental uncertainty, essentially the same as those determined using excitation at 710 nm. As shown in the top panel of Figure 5, the two energy transfer processes from the aggregated BChl *e* to the baseplate BChl *a* again exhibit a shifted DAS spectrum in the baseplate BChl *a* emission, which is better resolved in this case because the kinetics were detected with a smaller wavelength interval. In addition, the DAS shows a pronounced shoulder around 770 nm, where aggregated BChl *e* emits, not seen in the corresponding

DAS obtained upon excitation at 710 nm. This might indicate the presence of more than one BChl *e* pigment pool and incomplete excitation equilibration within the BChl *e* pools prior to the transfer to the baseplate.

For the Car-inhibited chlorosome, the global analysis of the kinetics measured upon excitation at 710 nm results in the DAS shown in the bottom panel of Figure 5. As observed for the control chlorosomes, two of the components are associated with the energy transfer from the aggregated BChl *e* to the baseplate BChl *a*, and the corresponding DAS components in the BChl *a* emission region again exhibit a spectral shift with respect to each other. Besides these similarities, differences from the control chlorosomes were found in two cases. First, the time constants for the energy transfer from aggregated BChl *e* to the baseplate are clearly longer, with values of 49 and 140 ps, respectively. Secondly, the relaxation of the equilibrated excitation between the baseplate BChl *a* and the aggregated BChl *e*, after arriving at the baseplate, is dominated by a component with a shorter lifetime of 400 ps. It therefore leads to an overall faster decay in comparison to that measured using the control chlorosomes at similar wavelengths.

Fluorescence lifetimes determined from the Car-inhibited chlorosomes upon excitation at 730 nm are in general shorter than the lifetimes determined using an excitation at 710 nm. As shown in the bottom panel of Figure 5, in the BChl *a* emission region, spectrally shifted DAS were found not only for the two components associated with the energy transfer processes, but also for the subsequent relaxation of the equilibrated excitations after their arrival in the baseplate.

Discussion

Efficiency of Car→BChl energy transfer

As reported by Arellano et al (2000), inhibition of Car biosynthesis affected the position and relative intensity ratio of the Soret and Q_y bands of BChl *e*. For this reason it is not possible to give an exact value of the Car→BChl energy transfer efficiency from the excitation spectra, but sufficiently precise estimate can still be made. The excellent agreement between

absorption and excitation spectra for Car-inhibited chlorosomes indicates that internal conversion from the Soret band to the Q_y band of BChl *e* has an efficiency close to 100%. It is reasonable to expect the same efficiency also for control chlorosomes and therefore the difference between 1-T and excitation spectrum of the control chlorosomes should result from a lower than 100% efficiency of Car→BChl energy transfer. An actual efficiency was estimated on the basis of (i) a comparison of the energy not transferred from Cars to BChls (calculated from the difference between absorption and fluorescence excitation spectra) versus the total energy absorbed by Cars in control chlorosomes (all spectra in wavenumbers and OD units) as well as from (ii) a comparison of the amplitude difference between absorption (1-T) and fluorescence excitation spectrum versus calculated absorption (1-T) of Cars at a given wavelength between 450-510 nm. Both approaches lead to the same conclusion that the efficiency of the Car→BChl energy transfer is between 60-70% in control chlorosomes. In both cases, the contribution of Cars was estimated on the basis of the experimentally confirmed expectation that the oscillator strength per BChl *e* molecule is the same for BChl *e* monomers (extracted to ethanol) and BChl *e* aggregates both in control and Car-inhibited chlorosomes. As no apparent difference was found for the excitation spectra detected by monitoring the fluorescence emission from BChl *e* and BChl *a*, the efficiency of the BChl *e*→ BChl *a* energy transfer must be close to 100% and/or (for control chlorosomes) the efficiency of Car→BChl *a* and Car→BChl *e* energy transfers must be similar. Also, we can conclude that 50-100 % (but not less) of the energy transferred from Cars to BChls is transferred to BChl *e*, assuming BChl *a*→BChl *e* backward energy transfer is negligible. However, the conclusion that the overall efficiency is 60-70% is valid only for the control chlorosomes used in this particular work. For other chlorosome preparations from *Chl. phaeobacteroides* substantial deviation between (1-T) and fluorescence excitation spectrum was observed by Aschenbrücker et al. (unpublished data), indicating only 15% efficiency of Car→BChl energy transfer. This conclusion was also supported by time-resolved data. It should be stressed that different strains of *Chl. phaeobacteroides* were used in the earlier

(Aschenbrücker et al.) and present work, which were cultivated under significantly different conditions. Aschenbrücker et al. used a strain 1549 grown in continuous culture under a light intensity of 25 μmol m^{-2} s^{-1} from an incandescent lamp, and in this work we used a strain CL1401 grown in batch culture under a light intensity of 100 μmol m^{-2} s^{-1} from a fluorescent lamp. These differences can cause large changes in the pigment composition, resulting in significant differences in the absorption spectra of the chlorosomes isolated from these strains. The most striking difference is an increase of the absorption around 450 nm for the chlorosomes used in the earlier work. This 'excessive' absorption corresponds very well with absorption of the extracted Cars in hexane (not shown). In addition, a relative ratio of BChl *e* to Cars estimated from absorption spectra of a pigment extract in ethanol was 4:1 in the earlier work by Aschenbrücker et al. and 6:1 in this work. Further study is necessary to explain the different efficiencies of energy transfer from Cars in various strains of green bacteria grown under different conditions.

Pathways and dynamics of Car→BChl energy transfer

Although the absorption spectrum itself hardly gives any direct evidence for the absence of Cars in the Car-inhibited chlorosomes (Figure 1), due to different absorption of aggregated BChl *e* in the two types of chlorosomes (Arellano et al 2000), Car absence was indeed revealed by the excitation spectra. Furthermore, the lack of Cars can be readily observed in femtosecond TA spectra. The most apparent difference between the TA spectra measured for the two types of chlorosomes is an evolution of the ESA band peaking at ~590 nm in the spectra of control chlorosomes. This band is significantly reduced for the Car-depleted chlorosomes (Figure 2). As ESA of Cars is typically found in this spectral region, we can attribute this band to ESA from the S_1 state of Cars. This attribution is also supported by the following characteristics of the kinetics measured within this band. (i) The kinetics measured using control chlorosomes exhibit a dominant decay component with a lifetime of ~10 ps, which is typical for the S_1 state of Cars with 9 conjugated double bonds (as isorenieratene,

ignoring the ring system) in organic solvents without energy transfer, e.g. β-carotene (Andersson et al. 1995). It therefore indicates that the S_1 state of Cars in the control chlorosomes can not be significantly involved in energy transfer, otherwise its lifetime should be substantially shortened. The same conclusion (and very similar lifetimes of the S_1 state) was reached also for the chlorosomes used in the previous work by Aschenbrücker et al. (unpublished data). Aschenbrücker et al. further showed that the extracted Car mixture and the native chlorosomes exhibit very similar lifetimes of the Car S_1 state. Most probabbly, the negligible involvement of the Car S_1 state in energy transfer is the result of the S_1 state being dipole-forbidden. In such a case, singlet energy transfer cannot occur via Förster mechanism. (ii) The overall amplitude of the kinetics measured for Car-inhibited chlorosomes is more than 3 times smaller due to the lack of Cars. It should be pointed out that the relatively small difference in the amplitudes of the TA signals measured at 580 nm between the two types of chlorosomes might be related with the 60-70% efficiency of energy transfer from Cars in the control chlorosomes. As the S_1 state is not active in energy transfer, it must be the S_2 state which is responsible for the most of the transferred energy. As discussed below, this leads to a shortening of the S_2 state lifetime and an inefficient population of the S_1 state of Cars. (iii) The kinetics measured for Car-inhibited chlorosomes decay slowly compared to those measured at the same pump/probe wavelength using the control chlorosomes, although the much smaller amplitude and lower signal/noise ratio of the kinetics make it hard to exactly evaluate the fitting parameters. The origin of this weak ESA signal between 560-630 nm for Car-inhibited chlorosomes is not clear. It may be due to the ESA of remaining Cars and/or BChl *e* (with maximum at 670 nm).

To obtain information about an involvement of Car S_2 state in Car→BChl energy transfer observed in the excitation spectra, we now concentrate on the spectral region 510-560 nm. The PB/SE band dominating TA spectra in this part has its maximum at ~540 nm and is attributed to the PB/SE of the BChl Soret band which is, in the case of control chlorosomes, mixed with an additional contribution from Cars. This conclusion is supported by the fact that amplitudes of the kinetics probed within this PB/SE band, after normalizing by

the number of absorbed photons, are essentially the same for both chlorosomes. It therefore means that the photons absorbed by Cars also contribute to the TA changes in control chlorosomes. As this PB/SE band is ~20 nm red shifted from the corresponding maximum of steady-state absorption spectra, SE must contribute to the TA spectra to a large extent. The TA spectra reveal substantially faster decay of this band for control chlorosomes. The initial decay of the kinetics probed within 510-560 nm using both chlorosome preparations is characterized by a time constant around 50 fs. For the inhibited chlorosomes this fast decay should reflect mainly the rapid relaxation within/from the Soret band, and an additional fast contribution from Cars is expected for the control ones. Except the similarity in the time constant, there is a clear difference in the corresponding amplitudes: For the Car-depleted chlorosome at 540 nm the amplitude is less than 70% of that obtained for the control chlorosomes (Figure 3). We attribute the 'excessive' part of the amplitude associated with the ~50 fs decay resolved using the control chlorosomes to the contribution from the Car S_2 state. Concerning the lifetime of this ultrafast decay component, it should be stressed once again that the cross-correlation was about 150 fs for this pump/probe wavelength combination and therefore the parameters of this ultrafast decay component could not be determined with a high accuracy. For the same reason we were not able to resolve the two independent sub-100 fs contributions from BChl and Car relaxation on the basis of their lifetimes. Despite these limitations, the initial decay is definitely substantially shorter than 100 fs. The significant shortening of the Car S_2 state under 100 fs can be explained by an ultrafast energy transfer from the S_2 state of Cars. As an involvement of the Car S_1 state in the energy transfer is unlikely, the pathway originating from the S_2 state should account for the ~60-70% efficiency of Car$\rightarrow$BChl energy transfer, as observed in the excitation spectra. This conclusion is supported by an estimate of the *in vivo* S_2 lifetimes of Cars. The *in vitro* S_2 lifetime of β-carotene, which has 9 conjugated double bonds (ignoring the ring system) as does isorenieratene, was determined previously by Macpherson and Gillbro (1998) and a solvent dependent lifetime in the range of 120-177 fs was found. Taking its average as 150 fs

and the 60-70% Car→BChl transfer efficiency, we calculated that the transfer time should be 65-100 fs. Our calculations also show that such a transfer process leads to a shortening of the S_2 lifetime to 45-60 fs, which is in good agreement with the resolved lifetime.

The larger amplitude of the ~50 fs component observed for control chlorosomes might be alternatively explained as an artifact due to the probe wavelength being close to the isosbestic point, which is 7 nm blue shifted at 500 fs delay time compared to the Car-depleted chlorosomes (Figure 2). However, this possibility seems to be unlikely, because the amplitude of the ultrafast component is significantly larger for control chlorosomes at all probe wavelengths between 510-560 nm, i.e. also at wavelengths far from the isosbestic point. Most importantly, the maximal difference in the amplitude of the ultrafast decay component between the two types of chlorosomes was not found at 565 nm, which is very close to the isosbestic point, but instead at around 540 nm (Figure 2).

Effect of Car inhibition on the dynamics of BChls

The slower decay components of the kinetics observed within the PB/SE region (τ_2 and τ_3 in Table 1) and the ESA band peaking around 680 nm and 670 nm for control and Car-deficient chlorosomes, respectively, are supposed to reflect mainly TA changes of BChl *e*. In both cases pronounced dependence of decay lifetime on the pump-intensity was observed, in comparison to those kinetics that are contributed to a large extent by Cars. The dependence on the pump intensity was found to be a good method to distinguish contributions from Cars (with weak dependence) and BChls (with strong annihilation) at all detection wavelengths and indicates that Cars are not in close mutual interaction, in contrast to BChls. Further, we noticed that if third (690 nm) or fourth (540 nm) decay component are introduced into the fitting for kinetics measured at low pump intensities, the lifetimes associated with the two longest components are very similar to the values determined from the kinetics measured in the Q_y band (Table 1). In addition, the ratio between the amplitudes of the 17-20 ps and 82-101 ps components is ~3 times higher for the control chlorosomes at 540 nm as well as in the Q_y band. All these facts lead to a conclusion that relatively slow relaxation both within the

PB/SE and ESA bands are due to relaxation within the Q_y band of the dominant BChl *e*, after initial relaxation from the Soret band and/or energy transfer from Cars. The minor component observed within the PB/SE band (τ_2, Table 1) might reflect vibrational relaxation within the Soret band. The assignment of the ESA band in the region from 640 to 690 nm to BChl *e* is also supported by the following reasons. First, the ESA of the aggregated chlorosomal BChls can be found typically in the blue part of the corresponding Q_y steady-state absorption band. This is true for the positive maxima of both control and inhibited chlorosomes, which in addition are mutually shifted by ~10 nm, similarly as respective absorption maxima of their BChl *e* Q_y bands. Secondly, kinetics measured within this spectral region begin with a rise significantly slower than found for the Car ESA. At 690 nm a ~0.5 ps rise time was resolved (Table 1).

The temporal evolution of the excited state relaxation of BChls in the spectral region between 700-810 nm was studied by TA and SPT. The use of SPT technique in this study is twofold: (i) to determine the lifetimes of these slow decay components which can not be well defined by TA due to its limited scan range and (ii) to avoid the effect of excitation annihilation. The latter is crucial for a large system with a dense arrangement of chromophores, typical for the aggregates in chlorosomes. Despite the fact, that SPT is restricted to spontaneous emission and TA contains three different contributions (PB, SE and ESA), the comparison of the results obtained by these two methods leads to the same conclusions. A common feature of the kinetics measured in the BChl Q_y region using the TA and SPT techniques is that two exponential components are required to fit both the decay of the aggregated BChl *e* and the rise of the baseplate BChl *a*. This observation is qualitatively consistent with the previous SPT measurement on a chlorosome preparation from the same species (van Walree et al. 1999), but the lifetimes resolved in that work are considerably different from what was found in the present study. The reason for this difference in the lifetimes might be the same as discussed under '*Efficiency of Car→BChl energy transfer*', given the fact that Aschenbrücker et al. (unpublished data) and van Walree at al. (1999) used the same strain and the growth conditions, both different from that used in this work. Different

growing conditions were reported to cause not only changes in pigment composition, but also a difference in the observed energy transfer rates (Fetisova at al. 1996). Both TA and SPT measurements also agree in generally slower energy transfer from the aggregated BChl *e* to the baseplate BChl *a* in Car-inhibited chlorosomes, although in TA the difference between BChl *a* rise times was rather small. Several possibilities may account for this difference in the transfer times obtained using the two types of chlorosomes. First, the change of spectral overlap between the emission of BChl *e* and absorption of BChl *a* for both types of chlorosomes would certainly affect the assumed Förster transfer rate between the donor and acceptor. However, despite the relatively large shift between the BChl *e* Q_y absorption bands of these two chlorosomes, their fluorescence emission spectra are shifted from each other by only 2 nm and therefore this possibility seems unlikely. More likely, a smaller baseplate and 30-40% decrease of BChl *a* observed for Car-inhibited chlorosomes (Arellano et al. 2000) may explain both the slower energy transfer and also the smaller amount of energy transferred to BChl *a*. The later is clearly visible in both TA and SPT data for the Car-depleted chlorosomes (Figure 4 and 5). Other possibilities include a variation in the spatial organization within aggregates and baseplate, as a slower subpicosend rise in BChl *e* was resolved by TA in Car-deficient chlorosomes, in addition to the obviously slower BChl *e* decay observed by both methods. This indicates less favorable energy transfer already within BChl *e* as a consequence of the Car inhibition. Our results thus support the idea of Car importance for optimization of both BChl a baseplate and BChl e aggregates. In the later case, Cars should affect BChl aggregates already during their formation since Car removal by hexane extraction does not substantially alter the BChl e organization (Aschenbrücker et al. unpublished data). The effect of Car inhibition on BChl e aggregates, which is manifested both in steady-state (Arellano et al. 2000) and time-resolved spectroscopy, can be either due to direct influence on the aggregate structure (e.g. orientation of dipole moments as suggested by Arellano et al. 2000) or due to so far not well understood effect of secondary BChl homologues, whose content is altered by Car inhibition, or BChl epimers.

Except above mentioned similarities, a number of differences in the lifetimes and

relative amplitudes of the resolved components were found in the results obtained by TA and SPT. (i) The faster decay component observed in BChl *e* region using TA experiments has a counterpart in a BChl *a* rise, and the lifetime (~19 ps) is approximately twice shorter than the corresponding 30-50 ps component obtained by SPT. (ii) The faster decay/rise component obtained by SPT experiment possesses the dominant amplitude, whereas in TA measurements the slower decay component dominates the relaxation of BChl *e* for both types of chlorosome. (iii) The dominant rise component of BChl *a* determined by TA measurements is remarkable slower than the corresponding decay component of BChl *e*. (iv) The decay of BChl *a* was observed to be slower for control chlorosomes than for Car-depleted ones in SPT experiment. This could not be confirmed in TA experiment due to the limited time window (600 ps). The differences given in (i-iii) may result from the fundamental difference between the two techniques and in the procedures used for the data analyses. First, due to the Stokes shift, which is exceptionally large in the case of BChl aggregates in chlorosomes (~30 nm for BChl *e*), we may at a given wavelength see a contribution from a different ensemble of molecules in TA and SPT experiment, respectively. This is because PB/SE and ESA contribute to the TA signal while in SPT experiment the signal is just from spontaneous emission. In this way, some processes observed by TA may remain hidden or have a different amplitude in SPT and vice versa. Secondly, the TA kinetics were analyzed by single decay fitting whereas the fluorescence decays measured using SPT were fitted by a global lifetime analysis at several wavelengths, which forces the lifetime to be identical at all detection wavelengths, and thus both the decay of BChl *e* and rise of BChl *a* were characterized by the same lifetimes. Although there are some difference in the results determined by TA and SPT, we would like to emphasis that both of these time-resolved techniques provide a clear evidence that two discrete time constants are required to describe the energy transfer processes from BChl *e* aggregates to BChl *a* and that Car inhibition lead to a slower energy transfer between BChls.

The detailed description of the relaxation processes within BChl *e* and BChl *a*, including the rise in BChl *e* and the subsequent energy transfer to BChl *a*, is the subject of a

forthcoming paper. To get the precise lifetime of the presumably sub-100 fs Car→BChl energy transfer, use of methods enabling an accurate determination of this parameter, like fluorescence up-conversion, is planned for the future. Further study of the reasons for the large differences in the efficiency of Car→BChl energy transfer observed for the two strains of one bacterial species grown under different conditions is necessary to understand the function of Cars in green bacteria properly.

Acknowledgment

This research was supported by the Swedish Natural Science Research Council, the EU TMR project "Green Bacterial Photosynthesis" (Grant No FMRX-CT96-0081) and the Kempe Foundation. J. Psencik also thanks to the Swedish Institute for financial support.

References

Andersson PO, Bachilo SM, Chen R-L and Gillbro T (1995) Solvent and temperature effects on dual fluorescence in a series of carotenes-energy-gap dependence of the internal-conversion rate. J Phys Chem 99: 16199-16209.

Arellano JB, Psencik J, Borrego CM, Ma Y-Z, Guyoneaud R, Abella CA, Garcia-Gil LJ and Gillbro T (2000) Effect of carotenoid biosynthesis inhibition on the chlorosome organization in *Chlorobium phaeobacteroides* strain CL1401. Photochem Photobiol 71: 715-723

Blankenship RE, Olson JM and Miller M (1995) Antenna complexes from green photosynthetic bacteria. In: Blankenship RE, Madigan MT and Bauer CE (eds) Anoxygenic Photosynthetic Bacteria, pp 399–435. Kluwer Academic Publishers, Dordrecht

Borrego CM and Garcia-Gil LJ (1995) Rearrangement of light harvesting bacteriochlorophyll homologues as a response of green sulfur bacteria to low light intensities. Photosynth Res 45: 21-30

Causgrove TP, Brune DC, Wang J., Wittmershaus BP and Blankenship RE (1990) Energy

transfer kinetics in whole cells and isolated chlorosomes of green photosynthetic bacteria. Photosynth Res 26: 39-48.

Causgrove TP, Brune DC and Blankenship RE (1992) Förster energy transfer in chlorosomes of green photosynthetic bacteria. J Photochem Photobiol B 15:171-179.

Fetisova ZG, Freiberg A, Mauring K, Novoderezhkin VI, Taisova AS and Timpmann K (1996) Excitation energy transfer in chlorosomes of green bacteria: Theoretical and experimental studies. Biophys J 71: 995-1010

Foidl M, Golecki JR and Oelze J (1997) Phototrophic growth and chlorosome formation in *Chloroflexus aurantiacus* under conditions of carotenoid deficiency. Photosynth Res 54: 219–226

Frese R, Oberheide U, van Stokkum I, van Grondelle R, Foidl M, Oelze J and van Amerongen H (1997) The organization of bacteriochlorophyll *c* in chlorosomes from *Chloroflexus aurantiacus* and the structural role of carotenoids and protein. An absorption, linear dichroism, circular dichroism and Stark spectroscopy study. Photosynth Res 54: 115–126.

Holzwarth AR, Müller MG and Griebenow K (1990) Picosecond energy transfer kinetics between pools in different preparations of chlorosomes from the green bacterium *Chloroflexus aurantiacus* Ok-70-fl. J Photochem Photobiol B 5: 457-465

Liaaen-Jensen S (1965) Bacterial carotenoids. XVIII. Aryl carotenoids from *Phaeobium*. Acta Chem Scand 19: 1025–1030

Ma Y-Z, Cox RP, Gillbro T and Miller M (1996) Bacteriochlorophyll organization and energy transfer kinetics in chlorosomes of *Chloroflexus aurantiacus* depend on the light regime during growth. Photosynth Res 47: 157–165

Macpherson AN and Gillbro T (1998) Solvent dependence of the ultrafast S_2-S_1 internal conversion rate of β-carotene. J Phys Chem A 102: 5049-5058.

Macpherson AN, Arellano JB, Fraser NJ, Cogdell RJ and Gillbro T (2001) Efficient energy transfer from the carotenoid S_2 state in a photosynthetic light-harvesting complex. Biophys J 80: 923–930

Melø TB, Frigaard NU, Matsuura K and Naqvi KR (2000) Electronic energy transfer involving carotenoid pigments in chlorosomes of two green bacteria: *Chlorobium tepidum* and *Chloroflexus aurantiacus*. Spectrochim Acta A 56: 2001-2010

Miller M, Cox RP and Gillbro T (1991) Energy transfer kinetics in chlorosomes from *Chloroflexus aurantiacus*: studies using picosecond absorbance spectroscopy. Biochim Biophys Acta 1057: 187-194

Mimuro M, Nishimura Y, Yamazaki I, Kobayashi M, Wang ZY, Nozawa T, Shimada K, Matsuura K (1996) Excitation energy transfer in the green photosynthetic bacterium *Chloroflexus aurantiacus*: A specific effect of 1-hexanol on the optical properties of baseplate and energy transfer processes. Photosynth Res 48: 263-270

Oelze J and Golecki JR (1995) Membranes and chlorosomes of green bacteria: Structure, composition, and development. In *Anoxygenic Photosynthetic Bacteria* (Edited by R. E. Blankenship, M. T. Madigan and C. E. Bauer), pp. 259–278. Kluwer Academic Publishers, Dordrecht.

Otte SCM, van der Heiden JC, Pfennig N and Amesz J (1991) A comparative study of the optical characteristics of intact cells of photosynthetic green sulfur bacteria containing bacteriochlorophyll *c*, *d* or *e*. Photosynth Res 28: 77-87

Prokhorenko VI, Steensgaard DB, Holzwarth AF (2000) Exciton dynamics in the chlorosomal antennae of the green bacteria *Chloroflexus aurantiacus* and *Chlorobium tepidum* Biophys J 79: 2105-2120

Psencik J, Searle GFW, Hala J and Schaafsma TJ (1994) Fluorescence detected magnetic resonance (FDMR) of green sulfur photosynthetic bacteria *Chlorobium* sp. Photosynth Res 40: 1–10

Psencik J, Vacha M, Adamec F, Ambroz M, Dian J, Bocek J and Hala J (1994) Hole burning study of excited state structure and energy transfer dynamics of bacteriochlorophyll c in chlorosomes of green photosynthetic bacteria. Photosynth Res 42: 1-8

Psencik J, Polivka T, Nemec P, Dian J, Kudrna J, Maly P and Hala J (1998) Fast energy transfer and exciton dynamics in chlorosomes of green sulfur bacterium *Chlorobium tepidum.* J Phys Chem A 102: 4392-4398.

Savikhin S, van Noort PI, Zhu Y, Lin S, Blankenship RE and Struve WS (1995) Ultrafast energy transfer in light-harvesting chlorosomes from the green sulfur bacterium *Chlorobium tepidum*. Chem Phys 194: 245-258

Savikhin S, Zhu YW, Blankenship RE and Struve WS (1996) Intraband energy transfers in the BChl *c* antenna of chlorosomes from the green photosynthetic bacterium *Chloroflexus aurantiacus*. J Phys Chem 100: 17978-17980

Savikhin S, Zhu YW, Blankenship, RE and Struve WS (1996) Ultrafast energy transfer in chlorosomes from the green photosynthetic bacterium *Chloroflexus aurantiacus.* J Phys Chem 100: 3320-3322

Schmidt K (1980) A comparative study on the composition of chlorosomes (*Chlorobium* vesicles) and cytoplasmic membranes from *Chloroflexus aurantiacus* OK–70–fl and *Chlorobium limicola* f. *thiosulfatophilum* strain 6230. Arch Microbiol 124: 21–31.

Steensgaard DB, van Walree CA, Permentier H, Baneras L, Borrego CM, Garcia-Gil J, Aartsma TJ, Amesz J, Holzwarth AR (2000) Fast energy transfer between BChl *d* and BChl *c* in chlorosomes of the green sulfur bacterium *Chlorobium limicola*. BBA-Bioenergetics 1457: 71-80

van Dorssen RJ, Vasmel H and Amesz J (1986) Pigment organization and energy transfer in the green photosynthetic bacterium *Chloroflexus aurantiacus*. II. The chlorosome. Photosynth Res 9: 33–45.

van Noort PI, Zhu Y, LoBrutto R and Blankenship RE (1997) Redox effects on the excited-state lifetime in chlorosomes and bacteriochlorophyll *c* oligomers. Biophys J 72: 316-325

van Walree CA, Sakuragi Y, Steensgaard DB, Frigaard N-U, Cox RP, Holzwarth AR and Miller M (1999) Effect of alkaline treatment on bacteriochlorophyll a, quinones and

energy transfer in chlorosomes from *Chlorobium tepidum* and *Chlorobium phaeobacteroides* . Photochem Photobiol 69: 322-328

Wang J, Brune DC and Blankenship RE (1990) Effects of oxidants and reductants on the efficiency of excitation transfer in green photosynthetic bacteria. Biochim Biophys Acta 1015: 457-46

Table 1

$\lambda_{pump} \rightarrow \lambda_{probe}$ [nm] (signal)	chlorosomes	τ_1 [ps] (A_1)	τ_2 [ps] (A_2)	τ_3[ps] (A_3)	τ_4[ps] (A_4)
505→515 (PB/SE)	control	0.05 (77%)*	0.7 (10%)	9 (13%)	
	Car-depleted	0.05 (64%)*	0.9 (12%)	14 (24%)	
505→540 (PB/SE)	control	0.05 (57%)*	3.0 (17%)	34 (26%)	
		*0.05 (55%)**	*2.2 (15%)*	*18 (22%)*	*88 (8%)*
	Car-depleted	0.05 (39%)*	5.3 (21%)	59 (40%)	
		*0.05 (38%)**	*2.9 (14%)*	*17 (23%)*	*97 (25%)*
505→580 (ESA)	control	0.06(-94%)*	9.7 (88%)	124 (12%)	
	Car-depleted#	0.07 (-48%)*	13.6 (85%)*	119 (15%)*	
505→690 (ESA)	control	0.47 (-33%)*	2.1 (18%)	44 (78%)	
		*0.46 (-35%)**	*1.7 (16%)*	*19 (33%)*	*80 (51%)*
685→745 (PB/SE)	control	0.42 (-39%)	18.5 (37%)	82 (63%)	
675→735 (PB/SE)	Car-depleted	0.51 (-42%)	20.2 (16%)	101 (84%)	
685→810 (PB/SE)	control	1.0 (-4%)**	18.7 (-12%)	125 (-86%)	207 (100%)
675→810 (PB/SE)	Car-depleted#	0.9 (-2%)*) **)	19.3 (-11%)*	142 (-89%)*	221 (100%)*

Table 1. Fitting parameters for the two-color isotropic kinetics. Corresponding pump intensities are given in captions of Figure 3 and 4. Parameters in italics are from fits where four exponential components were used alternatively. Lifetimes were obtained with standard deviation below 10%, except those denoted by star (*). The component denoted by two star (**) was used to fit coherent-like spike at the beginning of the kinetics. #Parameters could not be determined with a sufficient accuracy due to a low signal-to-noise ratio

Figure Captions

Figure 1. Fluorescence excitation spectra (solid line) and 1-T (symbols) spectra of control (top) and Car-depleted (bottom) chlorosomes. The difference spectra are shown between 420-600 nm (dotted line; multiplied by 5 for clarity).

Figure 2. Transient spectra (-Δ OD) excited at 505 nm for control (top) and Car-depleted (bottom) chlorosomes. Pump intensity was $4 \cdot 10^{13}$ photons·cm^{-2}·pulse^{-1}, sample OD ~0.5 at the respective BChl *e* Q_y maximum.

Figure 3. Top panel: Isotropic kinetics (symbols) and their best fits (lines) for the control (squares) and Car-depleted (circles) chlorosomes pumped at 505 nm and probed at 540 nm (pump intensity $2 \cdot 10^{13}$ photons·cm^{-2}·pulse^{-1}, sample OD ~0.5 at the respective BChl *e* Q_y maximum). Inset shows the same data on extended time scale. Bottom panel: Isotropic kinetics (symbols) and their best fits (lines) for the control (squares) and Car-depleted (circles) chlorosomes pumped at 505 nm and probed at 580 nm (pump pulse intensity $4 \cdot 10^{13}$ photons·cm^{-2}·pulse^{-1}, sample OD ~0.5 at the respective BChl *e* Q_y maximum). Insets show first two picoseconds for control chlorosomes probed at 580 nm (left) and 690 nm (right).

Figure 4. Top panel: Isotropic kinetics (symbols) and their best fits (lines) for control (Car-depleted) chlorosomes pumped at 685 nm (675 nm) and probed at 745 nm (735 nm), respectively (pump intensity $7 \cdot 10^{11}$ photons·cm^{-2}·pulse^{-1}, sample OD ~1 at the respective BChl *e* Q_y maximum). Inset shows first two picoseconds. Bottom panel: Isotropic kinetics (symbols) and their best fits (lines) for control (Car-depleted) chlorosomes pumped at 685 nm (675 nm), respectively, and probed at 810 nm (pump intensity $7 \cdot 10^{11}$ photons·cm^{-2}·pulse^{-1}, sample OD ~3.5 at the respective BChl *e* Q_y maximum).

Figure 5. DAS obtained by global analysis of the fluorescence kinetics measured using the control chlorosome (top) and the Car-depleted chlorosomes (bottom) upon excitation at 710 nm. Insets show part of DAS upon excitation at 730 nm.

Figure 1

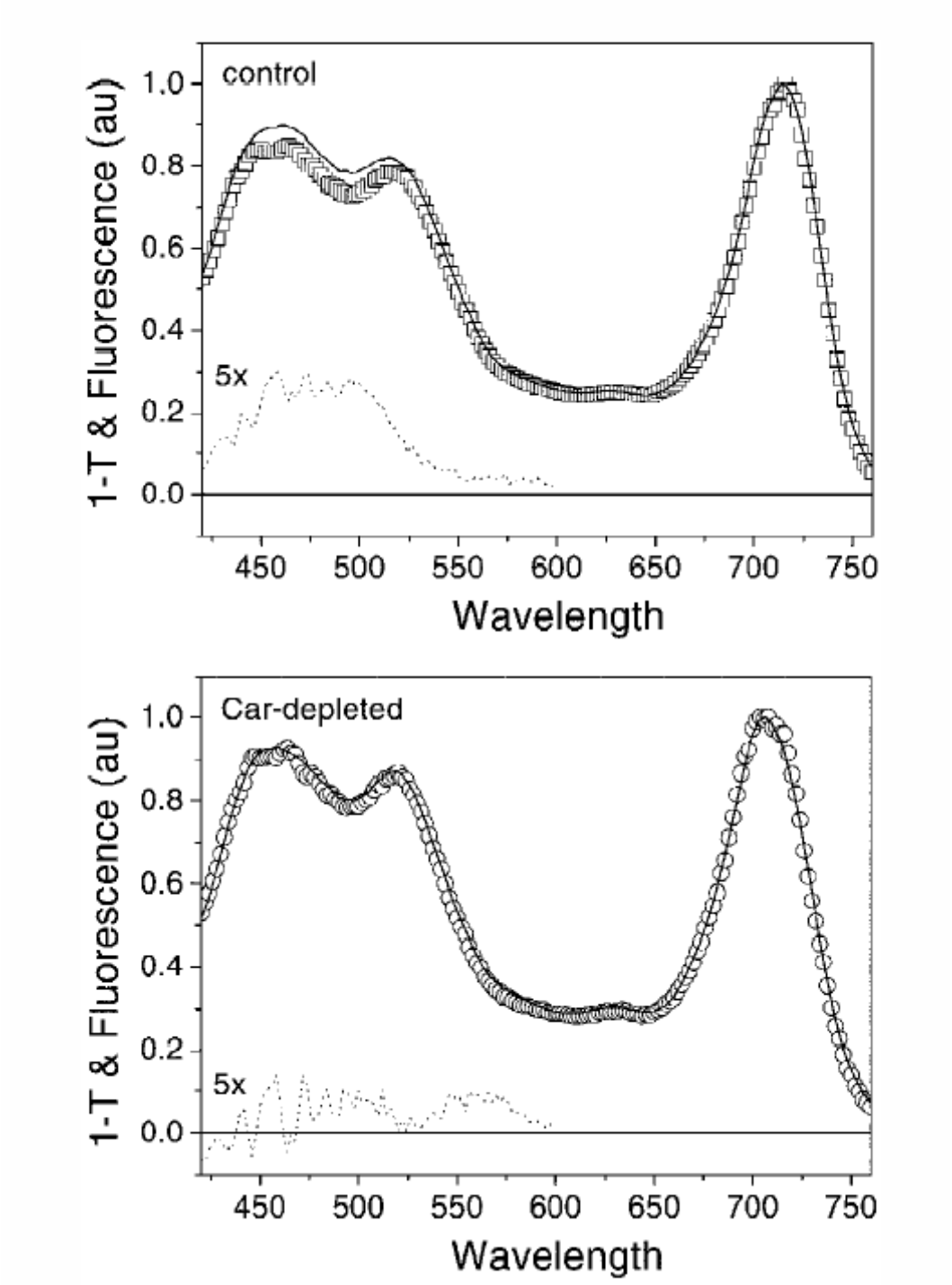
control
5x
1-T & Fluorescence (au)
Wavelength
Car-depleted
5x
1-T & Fluorescence (au)
Wavelength

Figure 2

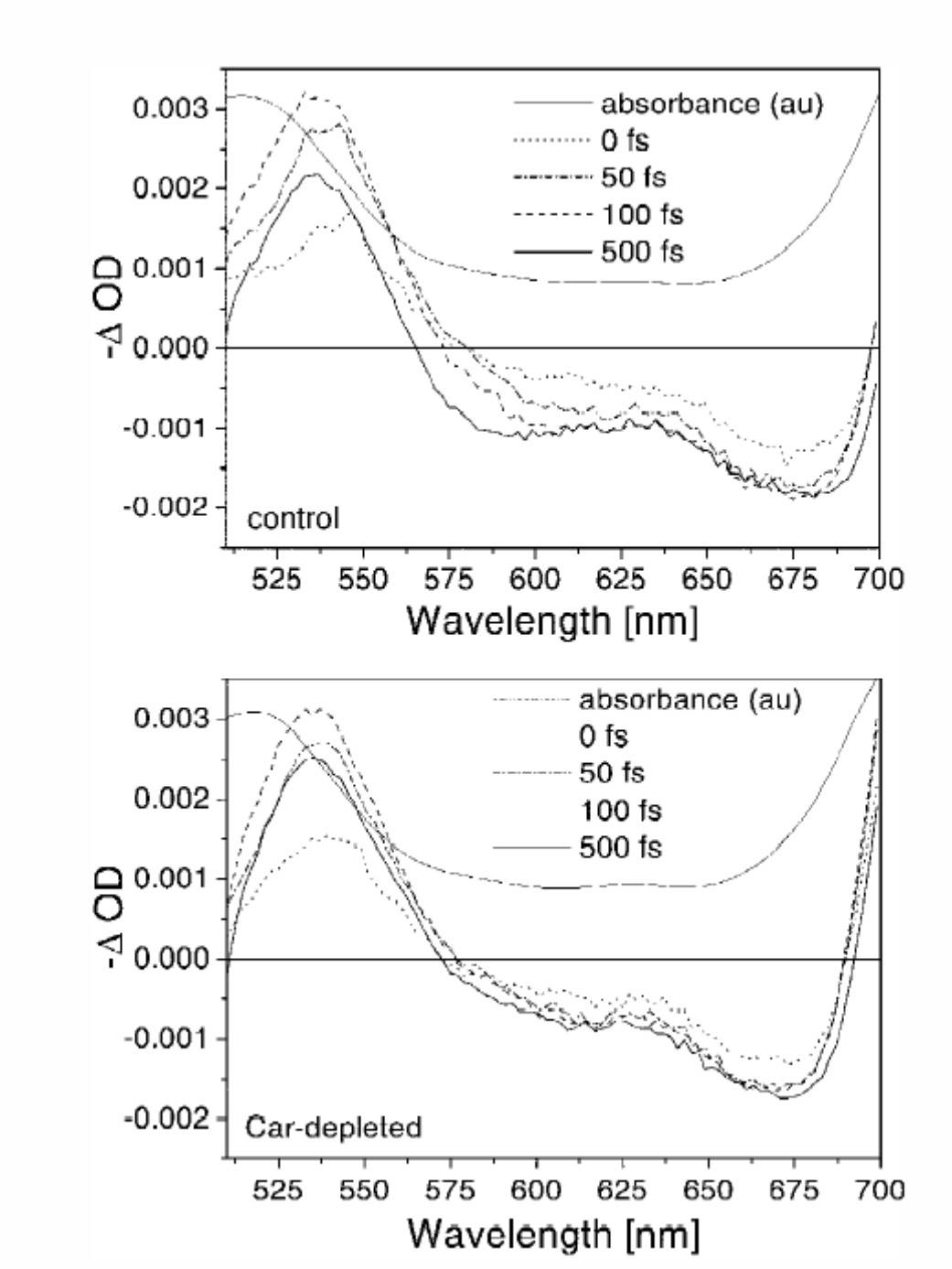
absorbance (au)
0 fs
50 fs
100 fs
500 fs
-Δ OD
0.003
0.002
0.001
0.000
-0.001
-0.002
control
525
550
575
600
625
650
675
700
Wavelength [nm]
absorbance (au)
0 fs
50 fs
100 fs
500 fs
-Δ OD
0.003
0.002
0.001
0.000
-0.001
-0.002
Car-depleted
525
550
575
600
625
650
675
700
Wavelength [nm]

Figure 3

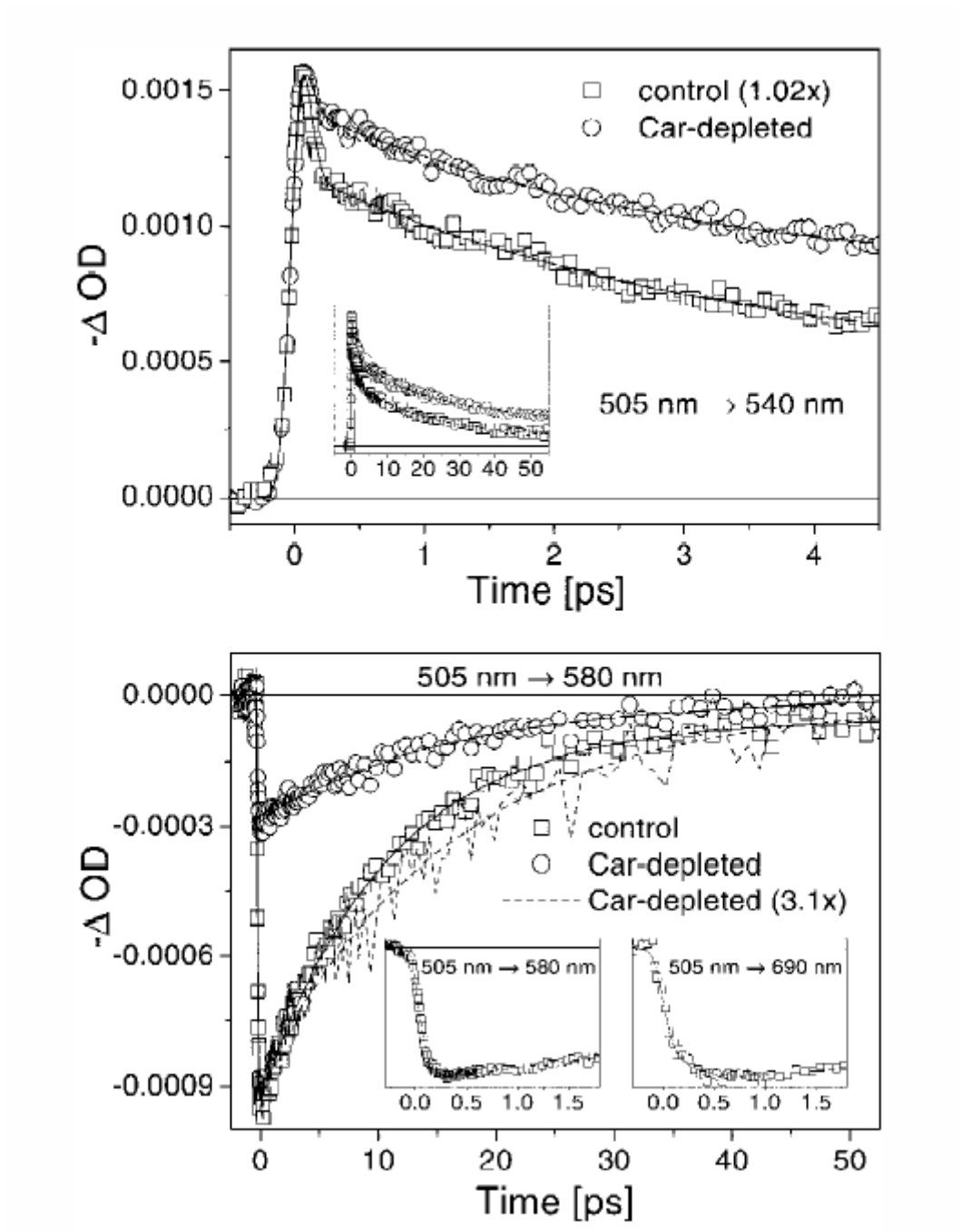
0.0015
0.0010
0.0005
0.0000
-Δ OD
control (1.02x)
Car-depleted
505 nm › 540 nm
0 10 20 30 40 50
0 1 2 3 4
Time [ps]
505 nm → 580 nm
0.0000
-0.0003
-0.0006
-0.0009
control
Car-depleted
Car-depleted (3.1x)
505 nm → 580 nm
505 nm → 690 nm
0.0 0.5 1.0 1.5
0.0 0.5 1.0 1.5
0 10 20 30 40 50
Time [ps]

Figure 4

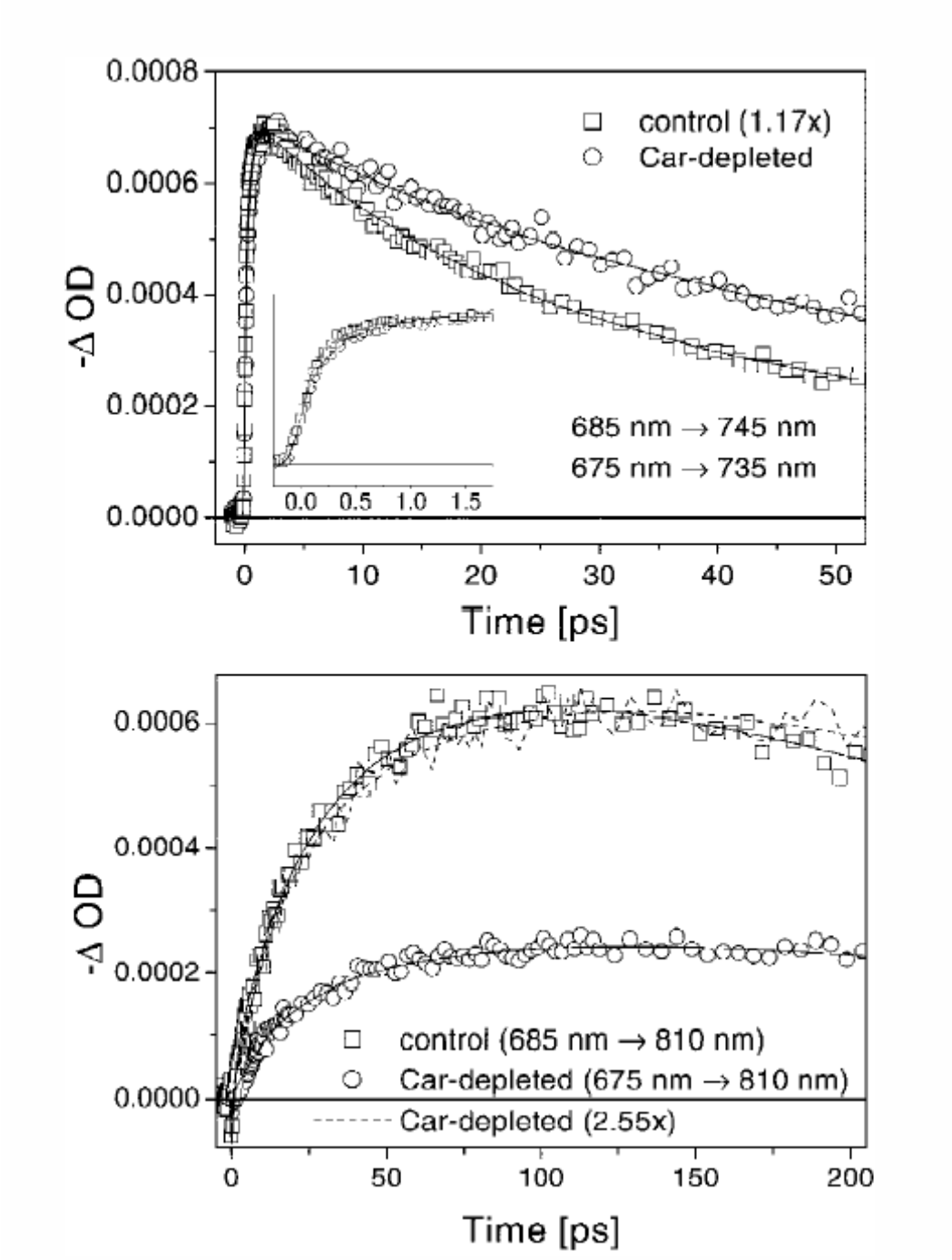
0.0008
0.0006
0.0004
0.0002
0.0000
-Δ OD
control (1.17x)
Car-depleted
685 nm → 745 nm
675 nm → 735 nm
0.0 0.5 1.0 1.5
0 10 20 30 40 50
Time [ps]
0.0006
0.0004
0.0002
0.0000
-Δ OD
control (685 nm → 810 nm)
Car-depleted (675 nm → 810 nm)
Car-depleted (2.55x)
0 50 100 150 200
Time [ps]

Figure 5

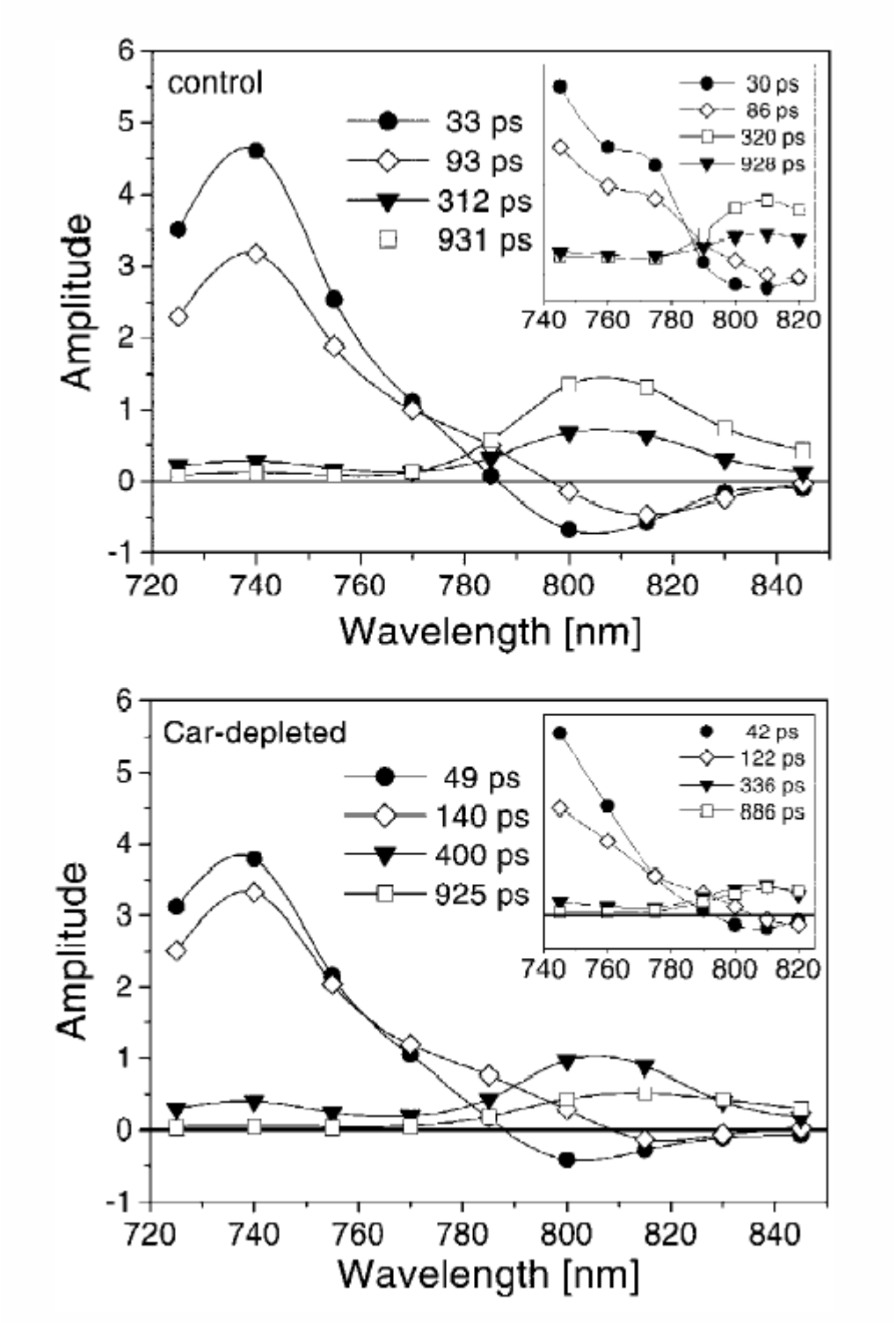
control
33 ps
93 ps
312 ps
931 ps
30 ps
86 ps
320 ps
928 ps
Amplitude
Wavelength [nm]
Car-depleted
49 ps
140 ps
400 ps
925 ps
42 ps
122 ps
336 ps
886 ps
Amplitude
Wavelength [nm]